CEAS-GNC-2022-010

CEAS EuroGNC 2022
"Conference on Guidance, Navigation and Control"
3-5 May 2022 @ Technische Universität Berlin, Germany

Decoupled parameter identification for a flexible aircraft

Sára Olasz-Szabó MSc student, Developer, Systems and Control Lab, Institute For Computer Science and Control, Eötvös Loránd Research Network, 1111, Budapest, Hungary. olasz-szabo.sara@sztaki.hu

Tamás Baár Research Associate, Systems and Control Lab, Institute For Computer Science and Control, Eötvös Loránd Research Network, 1111, Budapest, Hungary baar.tamas@sztaki.hu

Tamás Luspay Senior Research Fellow, Systems and Control Lab, Institute For Computer Science and Control, Eötvös Loránd Research Network, 1111, Budapest, Hungary. tluspay@sztaki.hu

ABSTRACT

The paper proposes a decoupled identification approach for determining unknown parameters of a flexible aircraft. The methodology relies on an input-output transformation designed to excite only certain parts of the dynamics. Accordingly, a simplified Single Input Single Output (SISO) model is obtained, where an additional disturbance term is introduced for the neglected dynamics. Besides being a SISO problem, the decoupling transformation also scales down the numerical complexity of the identification problem by reducing the dimension of the unknown parameter vector. A well-known output error minimization can then be carried out either in batch or in real-time operation, where the introduced error due to the neglected dynamics can be directly incorporated in the characterization of the parameter estimation's goodness through bounding ellipsoids. A comparative numerical example is given based on a reduced order linear time invariant (LTI) model of an experimental aircraft developed in the FLIPASED project.

Keywords: Parameter identification, Flexible aircraft, System decoupling

1 Introduction

Recent trends in aircraft design are pointing towards the increased usage of composite materials in order to reduce weight and accordingly the fuel consumption and emission. The development of such lightweight and high aspect ratio aircraft is now in the phase of experimental testing and accordingly reveals new challenges for system and control engineers [1, 2]. While the ultimate goal is to control flexible aircraft, other aspects of the problem need also be taken into consideration. Issues related to aeroservoelasticity are arising not only in the control design, but also in modeling, identification, estimation and fault detection.

The paper investigates the parameter identification of a control oriented model for a flexible aircraft. As it is common in the modeling toolchain, generally a high-fidelity model of the aircraft is constructed first, using finite element methods (FEM) [3]. The state-space representation can be then obtained by trimming, linearizing and residualizing the non-linear FEM dynamics at different airspeeds. Performing these steps lead to a set of Linear Time Invariant (LTI) models over the admissible flight envelope. Model reduction methodologies can be then applied for the high-dimensional LTI models to derive a low-order model, suitable for model based control design [4]. However, real world testing (either on the ground, or in flight, or both) is necessary in order to validate the models and eventually modify or update certain parameters, especially the ones related to the more complex, aeroelastic dynamics of the aircraft.

A few different approaches exist in this research field. [5] proposed a control oriented parameter identification for small flexible winged aircrafts. Three different methodologies have been proposed and tested: Prediction-Error Method (PEM), Frequency Domain Analysis (FREDA) and Output only Modal Identification. A linear state-space model was created and used as a basis of the parameter identification for the flexible modes of an experimental UAV. Flight test results have been also reported by using different input excitation.

In recent years the authors in [6] have investigated the problem from various perspectives. First a non-linear separable least squares algorithm was used for identification, which was then combined with a transfer function model. Later, frequency domain identification methods have been applied using maximum likelihood estimation, further refined by adopting an iterative form. More recently, instrumental variable method was combined with a variance matching method to obtain the parameters of the stochastic flutter model, formulated as an auto-regressive (AR) model.

We are following a similar way, and building on the Autoregressive representation with Exogenous terms (ARX) for the identification of the selected flutter subsystem. The novelty of the paper lies in an input - output transformation based simplification of the identification problem, which guarantee interactions with the targeted dynamics only, and reduces the system model to a SISO one. Besides these benefits, the number of estimated parameters are also reduced. Furthermore, we discuss in detail how to account for estimation errors arising from the residual effects from the suppressed dynamical part of the plant, providing a complete systematic framework.

The paper is organized as follows. The flexible aircraft model, which serves as a test bed during the evaluation of the proposed identification method is discussed in Section 2. It is followed by a brief overview of the decoupling transformation design for isolating the targeted dynamics in Section 3. Section 4 presents the details of the ARX based subsystem identification method, while the corresponding results are discussed in Section 5.

2 The Flexible Aircraft Model

A brief description of the mathematical model, used as a basis for the parameter identification is given in this section. It is taken from the FLIPASED ([2]) project, which investigates integrated aircraft design strategies for flexible aircraft. The modeling of such an aircraft relies on two fields of aerospace engineering: structural dynamics and aerodynamics. During the model development special attention was paid for the adequate modelling of the aircraft's flutter characteristic. Flutter is a dynamic instability resulting from the coupling of the wing's structural dynamics and the aerodynamic loads, and its suppression by active control is continuously gaining interest [7–10].

The **structural model** of this specific aircraft is based on a high fidelity finite element (FE) model, which possesses more than 600,000 nodes. The number of nodes is reduced by means of Guyan reduction, also called condensation, to less than 200 nodes. Although the number of nodes is reduced significantly the relevant dynamics with respect to aeroservoelasticity and flutter are still represented. The aircraft performs rigid body and flexible body motions. The non-linear rigid body motion is represented by the Newton-Euler equations of motion [3]. The external loads acting on the aircraft structure directly affect the rigid body dynamics [11]. The displacements due to the aircraft flexibility are assumed to be small, therefore linear elastic theory can be applied for the elastic motion.

The **aerodynamic** loads mainly contribute to the external loads acting on the aircraft structure. The lifting surfaces of the aircraft are discretized by several trapezoidal shaped panels, also called aerodynamic boxes. With potential theory, the vortex lattice method (VLM) for steady aerodynamics or the doublet lattice method (DLM) for unsteady aerodynamics ([11, 12]) can be utilized to determine the resulting forces and moments. More information on the aerodynamic modeling of this specific aircraft is given by [12].

The **aeroservoelastic model** of the UAV captures the interactions between the structural dynamics and aerodynamics. The deflection of the control surface actuators and airbrake actuators affect the aircraft aerodynamics, while the engine thrust acts on the structure. The aerodynamic characteristics of the aircraft are further influenced by environmental conditions like steady wind, gusts and turbulences. The aeroelastic representation of the aircraft dynamics is non-linear. Through linearization the dynamics can

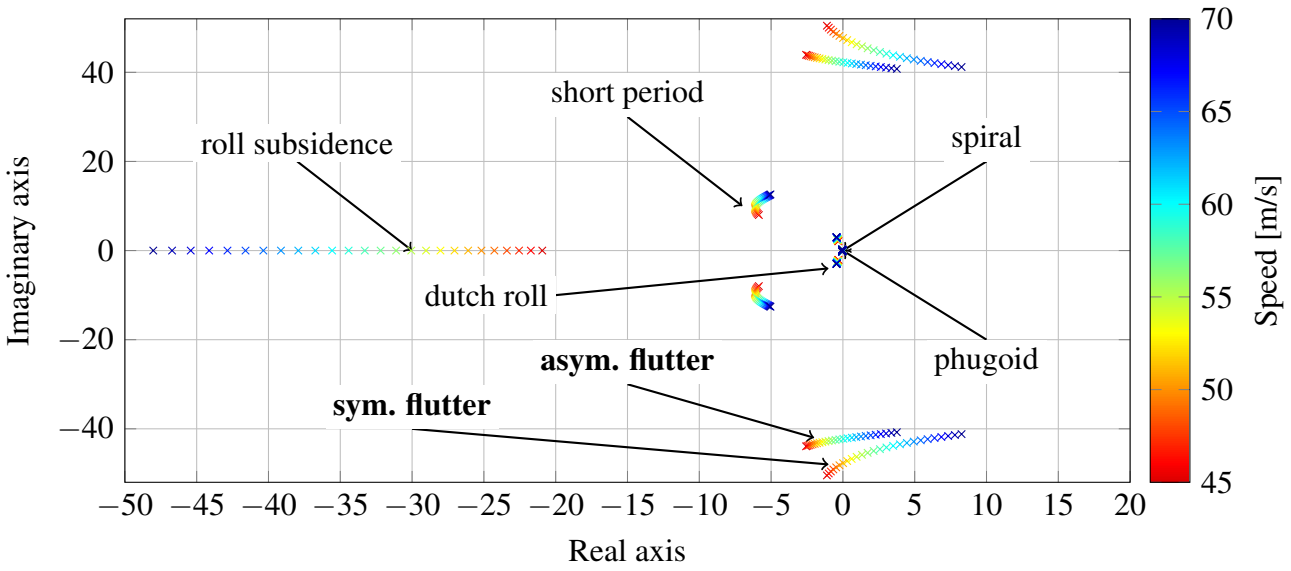

Fig. 1 The Pole-Zero map of the flexible wing aircraft

be represented by state-space systems in the form

$$\dot{x}(t) = Ax(t) + Bu(t) \quad (1)$$
$$y(t) = Cx(t) + Du(t). \quad (2)$$

Equation 1 defines the system dynamics and correlates the effect of the inputs $u(t)$ with the states $x(t)$. The modeled UAV is equipped with eight ailerons (four on the left and four on the right wings) and two ruddervators on each side. These inputs are used in the paper. Equation 2 provides the sensor dynamics, where the outputs $y(t)$ are the sensor measurements. For the subsystem identification problem we are using a special set of sensors. These are given at the 90% spanwise location on the left and right trailing edge, providing information about the vertical acceleration (a_z) and the angular rates (ω_x, ω_y) around the lateral and longitudinal axis of the aircraft respectively.

For more details about the modeling and control we refer to [13]. The obtained family of linear models is then transformed into a parameter varying modal form and a parameter varying model order reduction was performed [4]. The obtained low order model is given in its modal form and used for illustrating the proposed subsystem identification approach. Figure 1 then shows the pole migration map of the aircraft corresponding to (1) evaluated at various airspeed values, for a simplified illustration of the dynamic modes in the reduced system.

3 Decoupling of dynamical subsystems

The decoupling of dynamical systems is gaining more attention in the control community during the last couple of years. Here, we only present the main idea and key features of this approach, while the interested readers are invited to consult [14] and [15].

The main idea, which is applied for parameter identification in the paper is to isolate the flexible modes of the aircraft model from the remaining dynamics of the plant. This is achieved by suitable input and output transformations, called blending vectors. Consider a system which is given by the transfer function matrix:

$$G(s) = \sum_{i\in\{t,d\}} \left\{C_i(sI - A_i)^{-1}B_i\right\} + D = G_t(s) + G_d(s), \quad (3)$$

where for the ease of presentation we have arranged the subsystems into two groups. The targeted ones to be identified are in $G_t(s)$ while the remaining ones to be decoupled are in $G_d(s)$. The system's

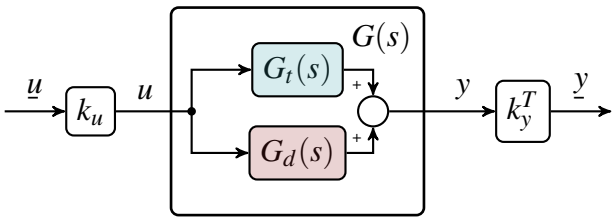

Fig. 2 Subsystem decoupling by input - output blends

state-space realization (1)-(2) is given with

$$A = \begin{bmatrix} A_t & 0 \\ 0 & A_d \end{bmatrix}, \quad B = \begin{bmatrix} B_t \\ B_d \end{bmatrix}, \quad C = \begin{bmatrix} C_t & C_d \end{bmatrix}, \quad D = \begin{bmatrix} D \end{bmatrix}. \tag{4}$$

As (4) suggests, the A matrix is block diagonal, where each block corresponds to one subsystem, therefore this representation is often referred as the modal form [16], where the eigenvalues of the blocks are the poles of the corresponding subsystems. Note that in (4), the dynamics are decoupled in A, however the input and output matrices (B and C respectively) are introducing a certain amount of coupling. With suitably designed input and output transformations we aim to reduce these interactions. For this the minimum and maximum sensitivities of these subsystem are used:

- the minimum sensitivity of a system is characterized by its $\mathscr{H}_-$ index, defined as

$$||G_t(s)||_- := \inf_{\omega} \underline{\sigma}\left[G_t(j\omega)\right], \tag{5}$$

  with $\underline{\sigma}$ denoting the minimum singular value.
- the maximum sensitivity of a system is characterized by its $\mathscr{H}_\infty$ norm, which is defined as

$$||G_d(s)||_\infty := \sup_{\omega} \bar{\sigma}\left[G_d(j\omega)\right], \tag{6}$$

  where $\bar{\sigma}$ denotes the maximum singular value.

Using the above system norms, it is possible to decouple the subsystems by introducing $k_u \in \mathbb{R}^{n_u \times 1}$ and $k_y \in \mathbb{R}^{n_y \times 1}$: the normalized (i.e., $\|k_u\| = \|k_y\| = 1$) input and output blending vectors [15]. These vectors transform the originally MIMO system into a SISO one (see Figure 2): the k_u input transformation simply redistributes a scalar input between the system's real physical inputs in a way that the excitation of targeted dynamics is maximized, while competing inputs cancel each other at the decoupled system's input. Similar reasoning applies for the k_y output transformation. For the computation of the blend vectors [15] proposed an Linear Matrix Inequality (LMI) based optimization, where $||k_y^T G_t(s) k_u||_-$ is maximized parallel with the minimization of $||k_y^T G_d(s) k_u||_\infty$.

4 Decoupled Parameter Identification

System identification in general deals with the problem of building mathematical models of a dynamical system based on observed data from the plant [17]. In the paper we have transformed the symmetric flutter mode into an Autoregressive Model with Exogenous Input (ARX), while the effect of the decoupled dynamics (i.e. rigid body and the asymmetric flutter mode) is modelled as a bounded disturbance. This formalism reduces the number of parameters to be estimated and also makes it possible to directly incorporate the decoupling transformation in the identification by using bounding ellipsoids.

Our starting point is the transfer function representation of the system, as given in (7). As discussed in the previous section, input and output transformations can be designed in order to decouple certain parts of the dynamics. In the present setup, we aim to excite the symmetric flutter mode of the system without interacting with the rest of the dynamics. Carrying out the numerical computations of [15] k_u

and k_y can be determined. Applying the blend vectors result in the following representation:

$$k_y^T G(s) k_u = \underbrace{k_y^T G_t(s) k_u}_{\overline{G}_t(s)} + \underbrace{k_y^T G_d(s) k_u}_{\overline{G}_d(s)}. \tag{7}$$

Due to the definition of the blending vectors the resulting subsystems (denoted by $\overline{G}_t$ and $\overline{G}_d$) are SISO. Moreover, the blend vectors are decoupling the two subsystems, which can be expressed as:

$$\left\|\overline{G}_d(s)\right\|_\infty << \left\|\overline{G}_t(s)\right\|_- . \tag{8}$$

Accordingly, the dynamics can be rewritten in the following ARX model structure [6]. Let the targeted and decoupled subsystems given as:

$$\overline{G}_t(q) = \frac{B_t(q)}{A_t(q)}, \quad \overline{G}_d(q) = \frac{B_d(q)}{A_d(q)}. \tag{9}$$

Here the introduced polynomials are expressed in the discrete time with the shift operator q as:

$$B(q) = (b_1 q^{-1} + b_2 q^{-2} + \cdots + b_{n_b} q^{-n_b}) q^{-n_k} \tag{10}$$

$$A(q) = 1 + a_1 q^{-1} + a_2 q^{-2} + \cdots + a_{n_a} q^{-n_a}, \tag{11}$$

where $B(q)$ and $A(q)$ the transfer function nominator and denominator, a_i and b_i are coefficients, n_a and n_b are orders of the polynomial, n_k is the dead-time of the system. The model output consist of two components

$$y(t) = y_t(t) + y_d(t), \tag{12}$$

where y, y_t and y_d are the model output, the symmetric flutter mode output and the decoupled subsystem output. Using the equations (10)-(12) one can construct the following:

$$y(t) = \frac{B_t(q)}{A_t(q)} u(t) + \frac{1}{A_t(q)} v(t) + \frac{B_d(q)}{A_d(q)} u(t) + \frac{1}{A_d(q)} v(t), \tag{13}$$

or equivalently:

$$y(t) = \overline{G}_t(q) u(t) + H_t(q) v(t) + y_d(t) \tag{14}$$

where $v(t)$ is a white noise and $H_t(q) = A_t(q)^{-1}$ [17] .

Introducing the standard definitions for the regressor vector $\varphi(t)$ and unknown parameter vector ϑ as follows:

$$\varphi(t) = [-y(t-1)\ -y(t-2)\ \ldots\ -y(t-n_a)\ u(t-n_k)\ u(t-n_k-1)\ \ldots\ u(t-n_k-n_b+1)]^T, \tag{15}$$

$$\vartheta = [a_1 \quad \ldots \quad a_{n_a} \quad b_1 \quad \ldots \quad b_{n_b}]^T, \tag{16}$$

(12) and the predicted output can be expressed as:

$$y(t) = \varphi^T(t)\vartheta + y_d(t) + \overline{v}(t), \tag{17}$$

where $\overline{v}(t) = H_t(q)v(t) + v_0(t)$, with $v_0(t)$ representing additional measurement noise. Consequently, the prediction error of the ARX model is written:

$$e(t) = y(t) - \hat{y}_t(t, \hat{\vartheta}) = A_t(q)y(t) - B_t(q)u(t), \tag{18}$$

where we have used the fact that:

$$\hat{y}_t(t, \hat{\vartheta}) = \frac{\overline{G}_t(q)}{H_t(q)} u(t) + \left(1 - \frac{1}{H_t(q)}\right) y(t) = B_t(q)u(t) + (1 - A_t(q))y(t). \tag{19}$$

The unknown ARX parameters can be then estimated by standard linear least squares (LS) techniques [17], where the optimal parameter vector is calculated:

$$\hat{\vartheta}_N = \left[\frac{1}{N}\sum_{i=1}^{N}\varphi(i)\varphi^T(i)\right]^{-1}\frac{1}{N}\sum_{i=1}^{N}\varphi(i)y(i) \tag{20}$$

where N is the number of available data samples. (20) can be used for computing the flexible parameters in batch mode, i.e. after gathering flight data and evaluating them off-line. As it is well known, the LS estimation can also be performed in real-time, by using recursive estimation.

In order to obtain the recursive formulas, (20) is usually rewritten into a matrix form with weighting exponential forgetting factor λ

$$\hat{\vartheta} = (\Phi\Lambda\Phi^T)^{-1}\Phi\Lambda Y, \tag{21}$$

where

$$\Phi = \begin{bmatrix}\varphi(1) & \cdots & \varphi(N)\end{bmatrix}, \quad Y = \begin{bmatrix}y(1)\\ \vdots \\ y(N)\end{bmatrix}, \quad \Lambda = diag\left(\lambda^{N-1},\cdots,\lambda^0\right). \tag{22}$$

Then the following algorithm is derived for the LS parameter estimation of the ARX model [17]:

$$\hat{\vartheta}(t) = \hat{\vartheta}(t-1) + K(t)\left[y(t) - \varphi^T(t)\hat{\vartheta}(t-1)\right], \tag{23}$$

$$K(t) = \frac{P(t-1)\varphi(t)}{\lambda(t) + \varphi^T(t)P(t-1)\varphi(t)}, \tag{24}$$

$$P(t) = \frac{1}{\lambda(t)}\left[P(t-1) - \frac{P(t-1)\varphi(t)\varphi^T(t)P(t-1)}{\lambda(t)+\varphi^T(t)+\varphi^T(t)P(t-1)\varphi(t)}\right]. \tag{25}$$

If one investigates the properties of the parameter estimation, then unbiased and convergent estimation of the real value is crucial. Rewriting (20) with the help of (12) the following can be obtained:

$$\begin{aligned}\hat{\vartheta}_N &= \left[\frac{1}{N}\sum_{i=1}^{N}\varphi(i)\varphi^T(i)\right]^{-1}\frac{1}{N}\sum_{i=1}^{N}\varphi(i)\left(\varphi^T(i)\vartheta + y_d(i) + \overline{v}(i)\right) = \\ &= \vartheta + \left[\frac{1}{N}\sum_{i=1}^{N}\varphi(i)\varphi^T(i)\right]^{-1}\frac{1}{N}\sum_{i=1}^{N}\varphi(i)\,y_d(i) + \left[\frac{1}{N}\sum_{i=1}^{N}\varphi(i)\varphi^T(i)\right]^{-1}\frac{1}{N}\sum_{i=1}^{N}\varphi(i)\overline{v}(i),\end{aligned} \tag{26}$$

where ϑ is the true parameter vector of the system. As it can be depicted, there are two terms in the above formula, which influence the unbiased estimation. The second term is standard in the system identification literature:

$$\left[\frac{1}{N}\sum_{i=1}^{N}\varphi(i)\varphi^T(i)\right]^{-1}\frac{1}{N}\sum_{i=1}^{N}\varphi(i)\overline{v}(i) \tag{27}$$

which is zero, if the inverse exists and if $\overline{v}(i)$ is a white noise seqeuence uncorrelated with $\varphi(i)$ every $i \in [1,N]$. The other term is related to the decoupled dynamics:

$$\left[\frac{1}{N}\sum_{i=1}^{N}\varphi(i)\varphi^T(i)\right]^{-1}\frac{1}{N}\sum_{i=1}^{N}\varphi(i)\,y_d(i). \tag{28}$$

However, y_d cannot be uncorrelated with the regressor vector φ due to the construction of the problem: the two subsystem is excited with the same input signal. Although condition (8) implies that $\|y_d\| << \|y_t\|$, i.e. the above term is almost zero, unbiased estimation cannot be guaranteed.

In order to characterize the bias, a bounding ellipsoid computation is given, based on [18]. The approach is to obtain a subspace of the parameter space which is compatible with the measurements and the effect of the decoupled subsystem, which is considered to be a disturbance. More precisely, we find an ellipsoid in the parameter space, whose center is the estimated parameter and which contains the real parameter vector ϑ.

In order to do so, we will start with an assumption on the energy of the disturbance signal as follows:

$$\sum_{i=1}^{t}(y_d(i)+\bar{v}(i))^2 \leq F(t), \tag{29}$$

which can be then rewritten as:

$$\|G_d(s)\|_\infty \sum_{i=1}^{t} u(i)^2 \leq F(t). \tag{30}$$

The above formula directly relates the achieved goodness of the decoupling (as discussed in the previous Section) with the goodness of the parameter estimation. In order to see this more clearly, the following is written:

$$\vartheta \in \Theta(t) = \{\vartheta : \sum_{i=1}^{t}(y(i)-\vartheta^T\varphi(i))^2 \leqslant F(t)\}, \tag{31}$$

where $\Theta(t)$ is the ellipsoid in which the true parameter lies if the energy constraint is satisfied. Furthermore, based on [18] the following form can be derived for the bounding ellipsoid:

$$\vartheta \in \Theta(t) = \{\vartheta : (\vartheta-\hat{\vartheta}(t))^T P(t)^{-1}(\vartheta-\hat{\vartheta}(t)) \leqslant G(t)\}, \tag{32}$$

where $\hat{\varphi}(t)$ and $P(t)$ is given by the recursive formulas, while $G(t)$ is

$$G(t) = F(t)+\hat{\vartheta}(t)^T P(t)^{-1}\hat{\vartheta}(t) - \sum_{i=1}^{t} y(i)^2 \tag{33}$$

$$= F(t)+\left(\sum_{i=1}^{t}\varphi(i)y(i)\right)^T P(t)\left(\sum_{i=1}^{t}\varphi(i)y(i)\right) - \sum_{i=1}^{t} y(i)^2 \tag{34}$$

using batch mode or:

$$G(t) = G(t-1)+(F(t)-F(t-1)) - \frac{(y(t)-\hat{\vartheta}(t-1)^T\varphi(t))^2}{1+\varphi(t)^T P(t-1)\varphi(t)} \tag{35}$$

in recursive estimation. Accordingly, the above formulas can be used for computing the bounding ellipsoids, which characterize the goodness of the parameter estimation. This information then can be directly used in state estimation, fault detection or control design by applying robust control methods.

5 System Identification Result

For the evaluation of the results, we aim to identify the symmetric flutter mode of the FLIPASED aircraft at 49 m/s airspeed value only and assume that rigid body dynamics and the asymmetric flutter mode parameters are known. This is certainly a simplified setup, however it illustrates the proposed methodology.

Before we discuss the numerical results, an important remark has to be taken. As discussed in Section 2, the modeling toolchain provides a mathematical model, which forms the basis of the analysis and synthesis. Throughout the paper we have assumed that nominal values of the parameters are given and can be used for computing the modal form and the blending vectors. If the real value differs significantly from the theoretic, nominal value, then both the modal form and the blending vector becomes inaccurate. As a possible remedy for this problem a robust decoupling algorithm has been developed

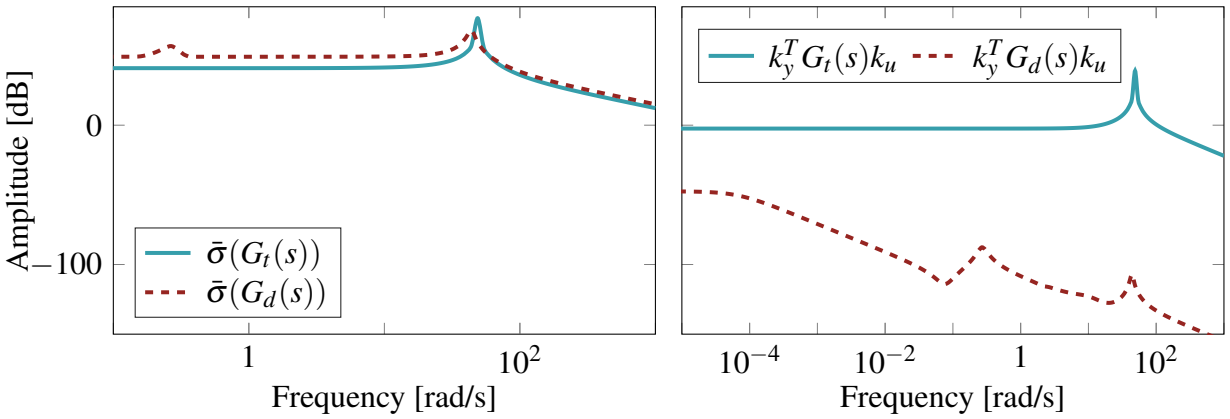

Fig. 3 The maximum singular values of the unblended, and the singular values of the blended subsystems

and currently under publishing [19] [20], where parameter uncertainties can be taken into consideration in the computation of the decoupling blend vectors.

5.1 Subsystem Decoupling

As it has been discussed in Section 3 the first step of the proposed subsystem identification algorithm is to find the suitable k_u and k_y input and output transformations, which decouple the targeted subsystem from the remaining dynamics. These blending vectors can be found by the algorithm given in [15], and so their numerical calculation is omitted here. However, their effect on the flexible aircraft model is represented in Figure 3. The left sub-figure depicts the maximum singular values of the original subsystems. Notice that the subsystem which should be decoupled has a higher transfer over the frequency range, i.e. certain inputs may excite this part of the dynamics more than the targeted one. This is especially true around the natural frequencies of the flutter modes (around 45 rad/s). In order to avoid the undesired interactions the proposed blend vectors are computed and applied to the system. The decoupling is shown in the right sub-figure of Figure 3, where it can be seen that the transfer through $k_y^T G_t(s) k_u$ is much higher over the complete frequency range than through $k_y^T G_d(s) k_u$. Note that the resonant peak corresponding to the asymmetric flutter mode is heavily suppressed, and given input signals may only excite the targeted dynamics. The obvious price that have to be paid for it, is the reduction of the sensitivity over the targeted subsystem.

5.2 Input Design

The reliable system identification data set is based on the input design. The input signals provide the excitation that is transmitted through the dynamic system and is measured in the output signals. As it is well known in the system identification literature, the input signals must contain sufficient energy at all frequencies of the system to be identified. Since every test flight in the development stage of the aircraft presents a risk, it is desired to minimize the number of tests and the complexity of the excitation signal for the flutter identification.

To meet these goals, a $3-2-1-1$ multistep input signal is proposed, as it is common in flight dynamics [21]. The $3-2-1-1$ input is $7 \times \Delta t$ long, where Δt is computed based on the ω_c natural frequency of the subsystem. For the underlying aircraft example, the nominal values of the flutter mode were used to compute the natural frequency as $\omega_c = 48.65$ rad/sec. From this information $\Delta t_{3211} \approx 0.3/\omega_c$ is derived and the $3-2-1-1$ signal is constructed by alternating positive and negative, equal-amplitude steps of relative duration 3, 2, 1 and 1. Furthermore, taking into consideration that the true flutter parameters differ from the nominal ones, two additional multistep signal was created with a 20% perturbation in ω_c. Figure 4 illustrates the power spectrum of the three signals, where it can be ssen that the highest excitation is achieved between 40 and 60 rad/sec.

In the simulations the parameter vector was set differently as the nominal one as given in Table 1 and additional white noise signals have been introduced at the model's output. The proposed sequence of input excitation consist of the three $3-2-1-1$ signal with control surface deflection of 4° and 20

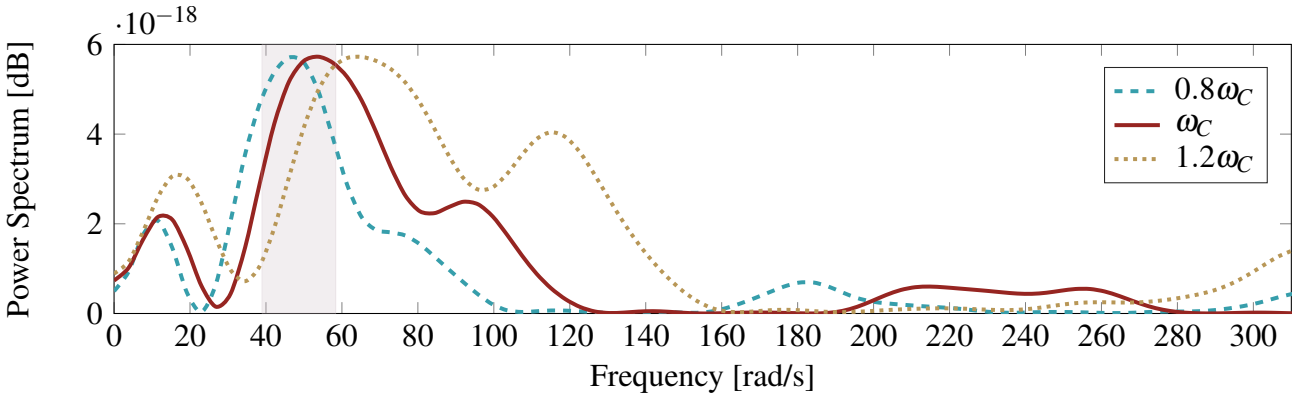

Fig. 4 The power spectrum of the designed input

seconds of pause between the signals. The signals were measured with $T_s = 0.01s$ sample time as in the real aircraft.

	$[a_{1_{ARX}}, a_{2_{ARX}}]$	poles
nominal system	$[-1.7597, 0.9907]$	$-0.4670 \pm 48.6497i$
true system	$[-1.6779, 0.9892]$	$-0.5442 \pm 56.6940i$

Table 1 Nominal and true system parameters and the corresponding flutter poles

The symmetric flutter mode consist of a complex conjugate pair of poles, therefore the following ARX model structure was selected

$$G_{ARX}(q) = \frac{B(q)}{A(q)} = \frac{b_{1_{ARX}} q^{-1} + b_{2_{ARX}} q^{-2}}{1 + a_{1_{ARX}} q^{-1} + a_{2_{ARX}} q^{-2}}. \tag{36}$$

Note that due to the decoupling, the dimension of the unknown parameter vector is significantly lower than a full system identification. The Recursive Least Squares algorithm presented in Section 4 is implemented to estimate the parameters. For initial parameters the nominal system's parameter was utilized and the forgetting factor was set to $\lambda = 1$.

t	$[a_{1_{ARX}}, a_{2_{ARX}}]$	J_a	poles	J_p [%]	J_{val}
1990	$[-1.6803, 0.9912]$	0.0032	$-0.4394 \pm 56.6361i$	0.2111	7.7771
3990	$[-1.6787, 0.9903]$	0.0014	$-0.4884 \pm 56.7089i$	0.1019	1.5411
5990	$[-1.6786, 0.9902]$	0.0012	$-0.4940 \pm 56.7106i$	0.0932	1.2984

Table 2 Decoupling system identification and validation results

Table 2 summarizes the results. The first column is the time index, where the three instances were chosen at the end of the 20 second intervals according to the multi-step input. The estimated parameters approach to the true value with each new excitation, as it can be read from the second column, or numerically evaluated by the following performance index in the third column:

$$J_a(t) = \sqrt{\sum_{1,2} (([a_{ARX_1}(t), a_{ARX_2}(t)]^T - [a_{ARX_{1_{true}}}, a_{ARX_{2_{true}}}]^T)^2)}.$$

In addition, the bounding ellipsoid has also been computed along with the recursive parameter estimation. Figure 5 illustrates the ellipsoids for the three time steps, along with their centers and the true value of the parameters. As one can depict, the size of the ellipsoid is shrinking over the time, giving a tighter bound on the possible real value of the parameter. Note also that the decoupling itself was successful

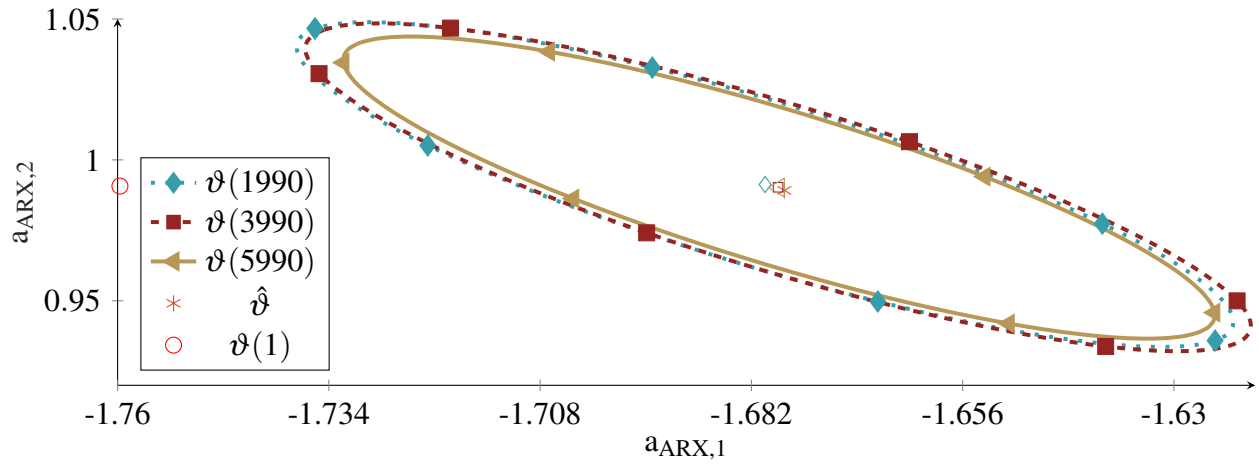

Fig. 5 Bounding ellipsoids

(see Figure 3) and accordingly the energy constraint on the disturbance was small. This is reflected in the small ellipsoids in Figure 5, where a maximum of 5% parameter deviation is predicted. From the estimated ARX parameters it is possible to calculate the poles of the system. These are referred as the flutter parameters (see the fourth column of Table 2), and their accuracy is characterized by the following cost function, numerically evaluated in the fifth column of the table:

$$J_p(t) = \frac{|p(t) - p_{true}|}{|p_{true}|}. \tag{37}$$

Lastly, a validating simulation has been carried out, where only the outer ailerons on each side have been used and the output of the original (i.e. without blend) system was compared with the estimated model. More precisely, a doublet signal was injected on the outer ailerons with the nominal ω_c frequency of the subsystem [21].

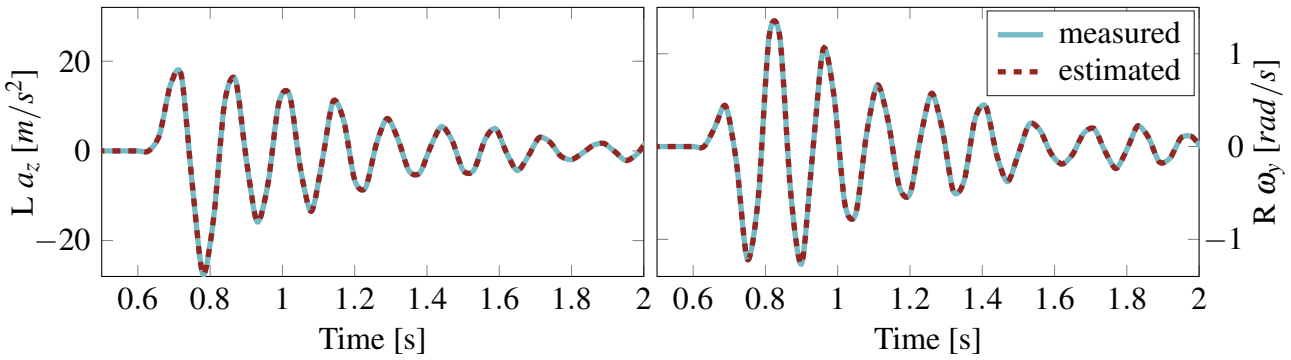

Fig. 6 Validation results (L: Left wing, R: Right wing)

Vertical acceleration measured at the left wingtip and the torsion of the right wing along the y axis is compared in Figure 6. It can be seen that the estimated parameters provide an accurate response. The squared error of the blended output was also computed as

$$J_{val}(t) = \sum_{outputs} \sum_{i=1}^{t} (y(i) - \hat{y}(i, \hat{\vartheta}(t)))^2, \tag{38}$$

and included in the last column of Table 2.

6 Conclusions and further research

A decoupled parameter identification is proposed in the paper for determining flexible model parameters for an UAV in the FLIPASED project. A decoupling approach was adopted first, where input and output transformations are computed and applied in order to excite only the targeted part of the dynamics. This step in itself carries two major benefits for system identification:

- the number of parameters is significantly reduced,
- the problem is converted into a SISO one, for which the exciting input design is simpler to calculate and implement.

The decoupled structure is then transformed into an ARX parameter estimation problem, where the effect of the decoupled dynamics are taken into account as an external, energy bounded disturbance signal. Accordingly, bounding ellipsoids on the estimated parameters are given along the recursive algorithm, characterizing the goodness of the estimation. A simulation example is given to illustrate and validate the proposed approach.

Our aim is to provide a simple, yet effective parameter identification tool for flexible aircrafts. In order to achieve this goal, the developed results have to be extended for non-linear dynamics as well, which will be in our research focus in the near future. Parameter-dependent identification approaches will be investigated. Furthermore, with successful simulation results in hand we will perform real flight tests and use the gathered data of the FLIPASED project.

Acknowledgments

The research leading to these results is part of the FLIPASED project. This project has received funding from the European Unions Horizon 2020 research and innovation programme under grant agreement No. 815058.

The research was supported by the Ministry of Innovation and Technology NRDI Office within the framework of the Autonomous Systems National Laboratory Program.

T. Luspay expresses his gratitude to Tsering Wangmo.

References

[1] FLEXOP project. Flutter Free FLight Envelope eXpansion for ecOnomical Performance improvement, 2015.

[2] FLIPASED project. FLight Phase Adaptive Aero-Servo-Elastic aircraft Design, 2019.

[3] Jeroen Hofstee, Thiemo Kier, Chiara Cerulli, and Gertjan Looye. A variable, fully flexible dynamic response tool for special investigations (varloads). In *International Forum on Aeroelasticity and Structural Dynamics*, 2003.

[4] Tamás Luspay, Tamás Péni, István Gőzse, Zoltán Szabó, and Bálint Vanek. Model reduction for LPV systems based on approximate modal decomposition. *International Journal for Numerical Methods in Engineering*, 113(6):891–909, 2018.

[5] Brian P Danowsky, David K Schmidt, and Harald Pfifer. Control-oriented system and parameter identification of a small flexible flying-wing aircraft. In *AIAA Atmospheric Flight Mechanics Conference*, page 1394, 2017.

[6] Hong Jianwang, Ricardo A. Ramirez-Mendoza, and Jorge de Lozoya Santos. Combing instrumental variable and variance matching for aircraft flutter model parameters identification. *Shock and Vibration*, (4296191):1–12, 2019.

[7] Bálint Patartics, Tamás Luspay, Tamás Péni, Béla Takarics, Bálint Vanek, and Thiemo Kier. Parameter varying flutter suppression control for the bah jet transport wing. *IFAC-PapersOnLine*, 50(1):8163–8168, 2017.

[8] Manuel Pusch, Daniel Ossmann, Johannes Dillinger, Thiemo M Kier, Martin Tang, and Jannis Lübker. Aeroelastic modeling and control of an experimental flexible wing. In *AIAA scitech 2019 forum*, page 0131, 2019.

[9] David K Schmidt, Brian P Danowsky, Aditya Kotikalpudi, Julian Theis, Christopher D Regan, Peter J Seiler, and Rakesh K Kapania. Modeling, design, and flight testing of three flutter controllers for a flying-wing drone. *Journal of Aircraft*, 57(4):615–634, 2020.

[10] Béla Takarics, Bálint Patartics, Tamás Luspay, Bálint Vanek, Christian Roessler, Julius Bartasevicius, Sebastian J Koeberle, Mirko Hornung, Daniel Teubl, Manuel Pusch, et al. Active flutter mitigation testing on the flexop demonstrator aircraft. In *AIAA Scitech 2020 Forum*, page 1970, 2020.

[11] T. Kier and G. Looye. Unifying manoeuvre and gust loads analysis models. In *International Forum on Aeroelasticity and Structural Dynamics*. American Institute of Aeronautics and Astronautics, 2009.

[12] Matthias Wuestenhagen, Thiemo Kier, Yasser M Meddaikar, Manuel Pusch, Daniel Ossmann, and Andreas Hermanutz. Aeroservoelastic modeling and analysis of a highly flexible flutter demonstrator. In *2018 Atmospheric Flight Mechanics Conference*, page 3150, 2018.

[13] Tamás Luspay, Tamás Péni, and Bálint Vanek. Control oriented reduced order modeling of a flexible winged aircraft. In *2018 IEEE Aerospace Conference*, pages 1–9. IEEE, 2018.

[14] Manuel Pusch and Daniel Ossmann. H_2-Optimal Blending of Inputs and Outputs for Modal Control. *IEEE Transactions on Control Systems Technology*, pages 1–8, 2019.

[15] Tamás Baár and Tamás Luspay. Decoupling through input–output blending. *International Journal of Control*, pages 1–15, 2020.

[16] Thomas Kailath. *Linear systems*, volume 156. Prentice-Hall Englewood Cliffs, NJ, 1980.

[17] L. Ljung. *System Identification: Theory for the User*. Prentice Hall information and system sciences series. Prentice Hall PTR, 1999.

[18] Eli Fogel. System identification via membership set constraints with energy constrained noise. *IEEE Transactions on Automatic Control*, 24(5):752–758, 1979.

[19] Tamás Baár and Tamás Luspay. Robust minimum gain lemma. In *Accepted for publication for the 2021 Conference on Decision and Control.* , 2021.

[20] Tamás Baár and Tamás Luspay. Robust decoupling of uncertain subsystems. *submitted to the International Journal of Robust and Nonlinear Control*, 2021.

[21] Ravindra V. Jategaonkar. *Flight Vehicle System Identification*, volume 216. American Institute of Aeronautics and Astronautics, 2006.